Title

Stemness factor Sall4 is required for DNA damage response in embryonic stem cells.

Journal

The Journal of cell biology, 208(5)

ISSN

0021-9525

Authors

Xiong, Jianhua
Todorova, Dilyana
Su, Ning-Yuan
et al.

Publication Date

2015-03-01

DOI

10.1083/jcb.201408106

Peer reviewed

Stemness factor Sall4 is required for DNA damage response in embryonic stem cells

Jianhua Xiong,[1]* Dilyana Todorova,[1]* Ning-Yuan Su,[1] Jinchul Kim,[1,3] Pei-Jen Lee,[2] Zhouxin Shen,[2] Steven P. Briggs,[2] and Yang Xu[1]

[1]Section of Molecular Biology and [2]Section of Cell and Developmental Biology, Division of Biological Sciences, University of California, San Diego, La Jolla, CA 92093
[3]Cancer Research Institute, Southern Medical University, Guangzhou 510515, Guangdong, China

Mouse embryonic stem cells (ESCs) are genetically more stable than somatic cells, thereby preventing the passage of genomic abnormalities to their derivatives including germ cells. The underlying mechanisms, however, remain largely unclear. In this paper, we show that the stemness factor Sall4 is required for activating the critical Ataxia Telangiectasia Mutated (ATM)–dependent cellular responses to DNA double-stranded breaks (DSBs) in mouse ESCs and confer their resistance to DSB-induced cytotoxicity. Sall4 is rapidly mobilized to the sites of DSBs after DNA damage. Furthermore, Sall4 interacts with Rad50 and stabilizes the Mre11–Rad50–Nbs1 complex for the efficient recruitment and activation of ATM. Sall4 also interacts with Baf60a, a member of the SWI/SNF (switch/sucrose nonfermentable) ATP-dependent chromatin-remodeling complex, which is responsible for recruiting Sall4 to the site of DNA DSB damage. Our findings provide novel mechanisms to coordinate stemness of ESCs with DNA damage response, ensuring genomic stability during the expansion of ESCs.

Introduction

As the origin of a multicellular organism, it is critical for pluripotent stem cells to establish stringent mechanisms to protect their genome from genetic mutations. In support of this notion, mouse embryonic stem cells (ESCs) harbor magnitudes lower frequency of genomic mutations than their differentiated derivatives (Hong et al., 2007; Tichy and Stambrook, 2008; Nagaria et al., 2013), but the precise mechanisms underlying this stringent genomic stability in ESCs are poorly understood. Electron microcopy and biochemical evidence have indicated that the introduction of double-stranded breaks (DSBs), a type of DNA damage naturally associated with cellular proliferation, induces dynamic chromatin epigenetics to facilitate the initiation and propagation of DNA damage response (DDR; Kim et al., 2009). However, considering the difference in the epigenetic landscape of ESCs and their differentiated derivatives (Meshorer and Misteli, 2006; Hong et al., 2007; Tichy and Stambrook, 2008; Nagaria et al., 2013), it remains unclear how DDRs are activated in ESCs to ensure genomic stability.

The *spalt* (*sal*) genes encode a family of highly conserved zinc finger proteins that are found in a great number of species as diverse as fruit fly, worm, and vertebrates (Sweetman and Münsterberg, 2006). In 1988, the homeotic gene *sal* was initially isolated and characterized in fruit fly (*Drosophila melanogaster*), where it is required for the homeotic specification in the embryonic termini (Frei et al., 1988; Jürgens, 1988). Beyond the invertebrates, its human homologues fall into four paralogues named Sall1–4, respectively. Sall4 is ubiquitously expressed in the embryo and especially in primitive inner cell mass. However, the distribution of Sall4 after birth is restricted to the adult stem/stemlike cells, preferentially in bone marrow and gonadal tissues (Sweetman and Münsterberg, 2006).

Sall4 is enriched in ESCs and is critical for maintaining the stemness of ESCs (Kohlhase et al., 2002; Koshiba-Takeuchi et al., 2006; Sweetman and Münsterberg, 2006; Yuri et al., 2009; Yang et al., 2012). Recent studies have highlighted that Sall4 could positively and negatively regulate gene expression through its interaction with the epigenetic machineries, such as

*J. Xiong and D. Todorova contributed equally to this paper.

Correspondence to Yang Xu: yangxu@ucsd.edu

J. Xiong's present address is the National Institutes of Health, Bethesda, MD 20892.

Abbreviations used in this paper: ATM, Ataxia Telangiectasia Mutated; ChIP, chromatin immunoprecipitation; CMV, cytomegalovirus; dsDNA, double-stranded DNA; DDR, DNA damage response; DOX, doxorubicin; DSB, double-stranded break; ESC, embryonic stem cell; ID, inside diameter; IR, ionizing radiation; MRN, Mre11–Rad50–Nbs1; MS, mass spectrometry; OD, outside diameter; SCX, strong cation exchange.

The Rockefeller University Press $30.00
J. Cell Biol. Vol. 208 No. 5 513–520
www.jcb.org/cgi/doi/10.1083/jcb.201408106

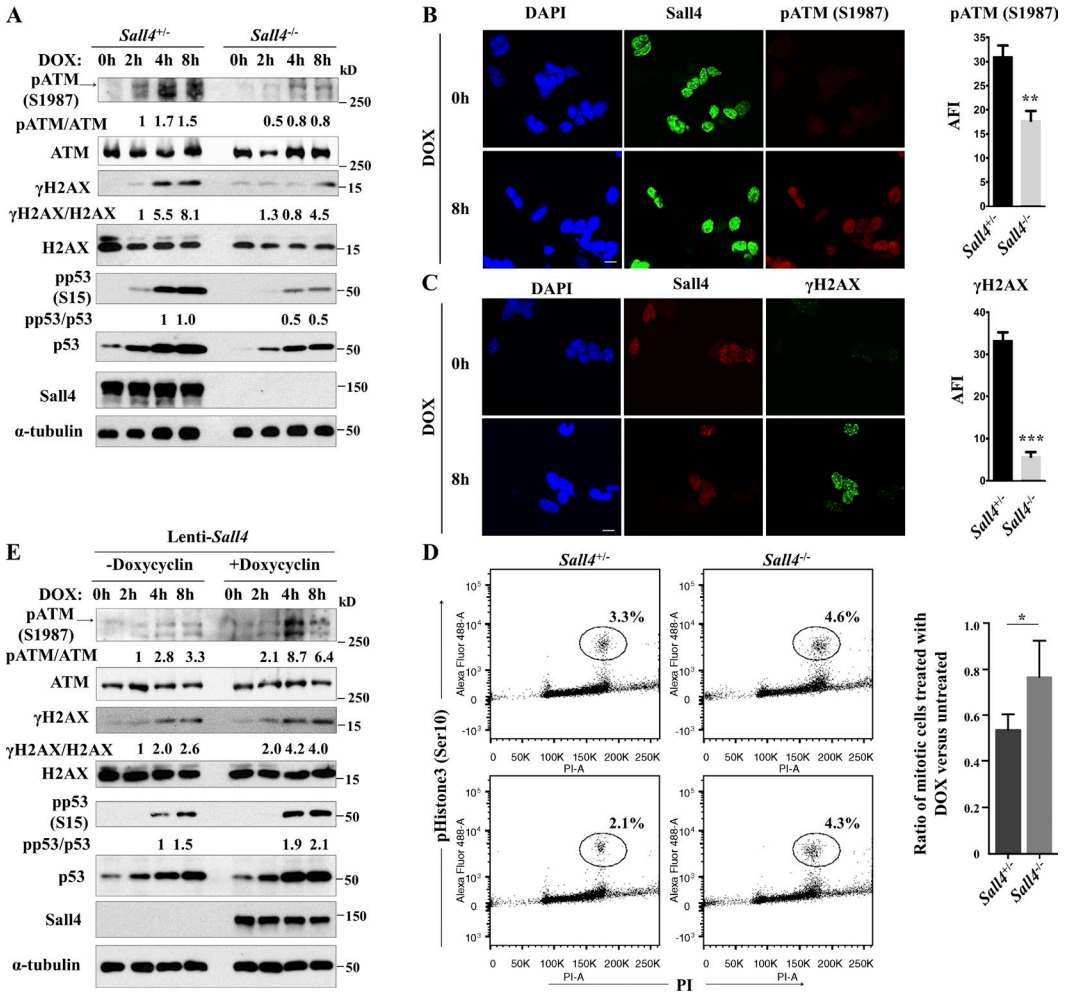

Figure 1. ***Sall4*$^{-/-}$ ESCs are impaired in ATM activation and hypersensitive to DOX treatment.** (A) Phosphorylation of ATM, H2AX, and p53 in *Sall4*$^{+/-}$ and *Sall4*$^{-/-}$ ESCs at different time points after DOX treatment. (B and C) *Sall4*$^{+/-}$ and *Sall4*$^{-/-}$ ESCs were mixed, treated with DOX or mock treated, and examined for the foci formation by ATM-Ser1987p (B) or γ-H2AX (C). DNA is counterstained with DAPI (blue). Bars, 10 µm. Graphs show the change of average fluorescence intensity (AFI) determined by dividing the overall mean fluorescence intensity by the area of the cell, and values are mean ± SEM. **, $P < 0.01$; ***, $P < 0.001$ by *t* test throughout the figure. (D) Cell cycle G_2/M checkpoint is impaired in *Sall4*$^{-/-}$ ESCs after DOX treatment. (top) Mock-treated control. (bottom) 1 h after after DOX treatment. The values are means ± SEM ($n = 4$). *, $P < 0.05$ by *t* test. Circles denote the percentages of cells positive for histone 3 phosphorylated at Ser10 in all cells. PI-A, propidium iodide area. (E) Inducible expression of Sall4 in *Sall4*$^{-/-}$ ESCs rescues the activation of ATM after DOX (0.5 µM) treatment. *Sall4*$^{-/-}$ ESCs were stably transfected with a doxycycline-inducible vector expressing ectopic Sall4 (Lenti-*Sall4*).

Mi-2/nucleosome remodeling and deacetylase complex and DNA methyltransferases (DNMTs), including DNMT1, DNMT3A, DNMT3B, and DNMT3L (Yang et al., 2012). Given the potential roles of Sall4 in extensive chromatin dynamics, we hypothesized that Sall4 might play a role in modulating epigenetics in ESCs in response to DNA damage.

Results and discussion

Sall4 is required for ATM activation in DDR in ESCs through its recruitment to DNA DSB sites

As Ataxia Telangiectasia Mutated (ATM) is the primary activator of the cellular responses to DNA DSB damage (Shiloh, 2003), we tested whether Sall4 is involved in ATM activation induced by DSB-inducing agent doxorubicin (DOX) in ESCs. The autophosphorylation of ATM at Ser1987 is a canonical marker of its activation in response to DSB alarm (Pellegrini et al., 2006). Therefore, we examined the ATM autophosphorylation in *Sall4*$^{+/-}$ and *Sall4*$^{-/-}$ mouse ESCs after DOX treatment, indicating that autophosphorylation of ATM at Ser1987 is significantly decreased in *Sall4*$^{-/-}$ ESCs when compared with *Sall4*$^{+/-}$ ESCs (Fig. 1, A and B). In support of the notion that ATM activation is impaired in *Sall4*$^{-/-}$ ESCs after DNA DSB damage, the phosphorylation of the ATM targets, including H2AX-Ser139p and p53-Ser15p, was also impaired in *Sall4*$^{-/-}$ ESCs after DNA damage (Fig. 1, A and C). Consistent with this finding, the levels of DNA damage were significantly higher in *Sall4*$^{-/-}$ ESCs than Sall4$^{+/-}$ ESCs after the treatment with DOX, indicating that DDR is defective in *Sall4*$^{-/-}$ ESCs (Fig. S1 A). In addition, the ATM-dependent G_2/M checkpoint was impaired in *Sall4*$^{-/-}$ ESCs after DOX treatment (Fig. 1 D). ATM activation is also impaired in *Sall4*$^{-/-}$ ESCs in response to DNA DSB damage induced by ionizing radiation (IR), further supporting the conclusion that Sall4 is required for efficient activation of ATM-dependent

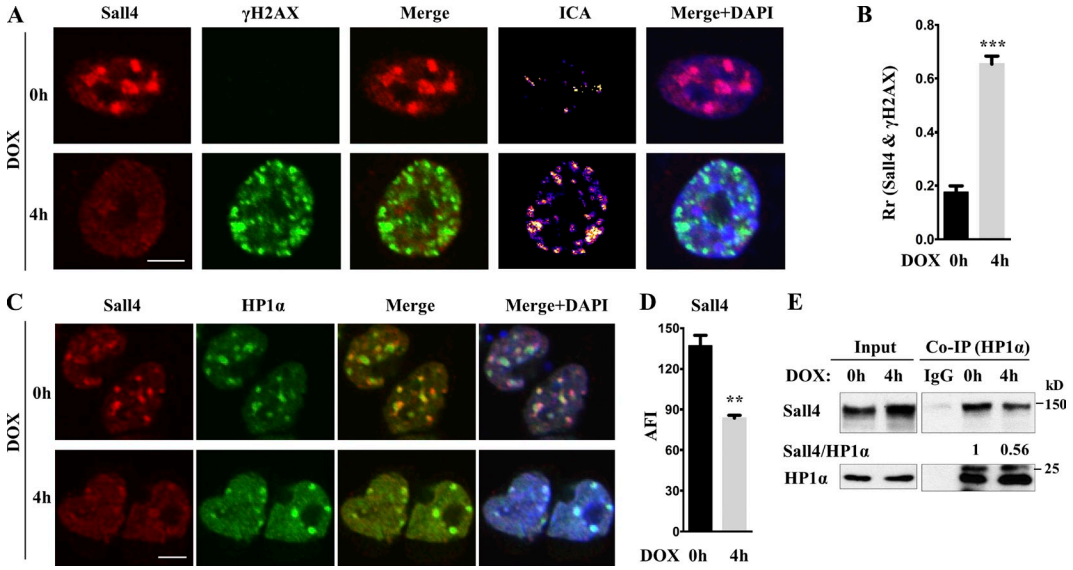

Figure 2. **Sall4 is relocated from the heterochromatin to DNA DSBs in ESCs after DOX treatment.** (A) Sall4 is sequestered in the heterochromatin and relocated to DNA DSBs in ESCs after DNA damage. *Sall4*$^{+/-}$ cells were examined for the foci formation of γ-H2AX and Sall4 before and after DNA DSB damage induced by DOX. Nuclei were counterstained with DAPI (blue). For intensity correlation analysis (ICA), pixels from the Sall4 channel covarying positively with the corresponding signal from the γ-H2AX or DAPI channel are denoted. Bar, 5 µm. (B) Rr analysis for the colocalization of Sall4 and γ-H2AX. Rr is the Pearson's correlation coefficient, and a value of 1 indicates perfect colocalization. The values of Rr are means ± SEM. ***, $P < 0.001$ by *t* test. (C) Sall4 is colocalized with HP1-α foci before DNA DSB damage and is mobilized out of HP1-α foci after DNA damage. Nuclei are counterstained with DAPI (blue). Bar, 5 µm. (D) The average fluorescence intensity (AFI) of Sall4 at heterochromatin was determined by dividing the overall mean fluorescence intensity by the area of the cell, and values are means ± SEM. **, $P < 0.01$ by *t* test. (E) DNA damage disrupts the interaction between Sall4 and HP1-α in ESCs. The interaction between Sall4 and HP1-α was analyzed by coimmunoprecipitation (Co-IP) with the HP1-α antibody.

responses to DNA DSB damage in ESCs (Fig. S1, B and C). In further support of this conclusion, *Sall4*$^{-/-}$ ESCs were hypersensitive to DNA DSB damage (Fig. S1 D).

To further confirm that the impaired ATM activation in *Sall4*$^{-/-}$ ESCs after DNA DSB damage is caused by the loss of Sall4, we used an inducible Lentiviral vector under the control of doxycycline to ectopically express Sall4 in *Sall4*$^{-/-}$ ESCs (Lenti-*Sall4*; Hockemeyer et al., 2008; Buganim et al., 2012). Doxycycline-induced expression of Sall4 in *Sall4*$^{-/-}$ ESCs rescued the phosphorylation of ATM at Ser1987 and phosphorylation of p53 at Ser15 (Fig. 1 E and Fig. S1 E) and rescued the hypersensitivity of *Sall4*$^{-/-}$ ESCs to DNA DSB damage (Fig. S1 D). These findings confirm that the impaired ATM-dependent DDRs in *Sall4*$^{-/-}$ ESCs are caused by the loss of Sall4.

To understand how Sall4 activates ATM after DNA DSB damage, we investigated whether Sall4 is recruited to the sites of DNA DSBs in ESCs. Consistent with previous findings of the direct binding of Sall4 to heterochromatin during transcription repression in ESCs (Sakaki-Yumoto et al., 2006), we showed that Sall4 is sequestered into the nuclear foci associated with DAPI-dense pericentric heterochromatin in ESCs before DNA damage (Fig. 2 A). In response to DNA damage, a substantial fraction of Sall4 was redistributed from the heterochromatin to the γ-H2AX foci formed around the site of DNA DSBs (Fig. 2, A and B). In further support of this notion, Sall4 protein diffused away from the heterochromatin marked by HP1-α (Fig. 2, C and D). This dynamic redistribution of Sall4 in ESCs after DNA damage is likely caused by its reduced affinity for heterochromatin because the interaction between Sall4 and HP1-α was significantly reduced in ESCs after DNA DSB damage (Fig. 2 E).

Sall4 and Baf60a are required for the recruitment and/or stabilization of MRN complex at the site of DNA damage

To understand the mechanism underlying the Sall4-dependent activation of ATM after DNA DSB damage, we used mass spectrometry (MS) to identify the proteins associated with Sall4 in ESCs (Fig. 3 A and Table S2). One of the Sall4-associated proteins identified by MS and confirmed by coimmunoprecipitation was Rad50, which serves as a key scaffold for the Mre11–Rad50–Nbs1 (MRN) complex linking DSBs to ATM signaling (Fig. 3 B and Table S2; Lee and Paull, 2007; Stracker and Petrini, 2011).

To investigate the functions of Sall4 in foci formation of Rad50, ATM, and γ-H2AX at the site of DNA DSBs, we examined the association of these proteins with DNA DSBs using DNA DSB pull-down assay as previously described (Song et al., 2007). Our findings demonstrate that the association between DNA DSBs with Rad50, Mre11, and Nbs1 was significantly reduced in *Sall4*$^{-/-}$ ESCs when compared with *Sall4*$^{+/-}$ ESCs (Fig. 3 C). Consistent with the finding that foci formation of phosphorylated ATM was impaired in *Sall4*$^{-/-}$ ESCs after DNA DSBs, the association of phosphorylated and total ATM with DNA DSBs was also significantly reduced in *Sall4*$^{-/-}$ ESCs (Fig. 3 C). These findings support the notion that Sall4 recruits and/or stabilizes the MRN complex at the site of DNA DSB damage, leading to ATM activation.

Accumulating evidence has indicated that chromatin structure around the DNA DSBs needs to be remodeled to grant the access of DNA repair proteins to DNA damage lesion. This could be achieved by two main mechanisms: (1) histone

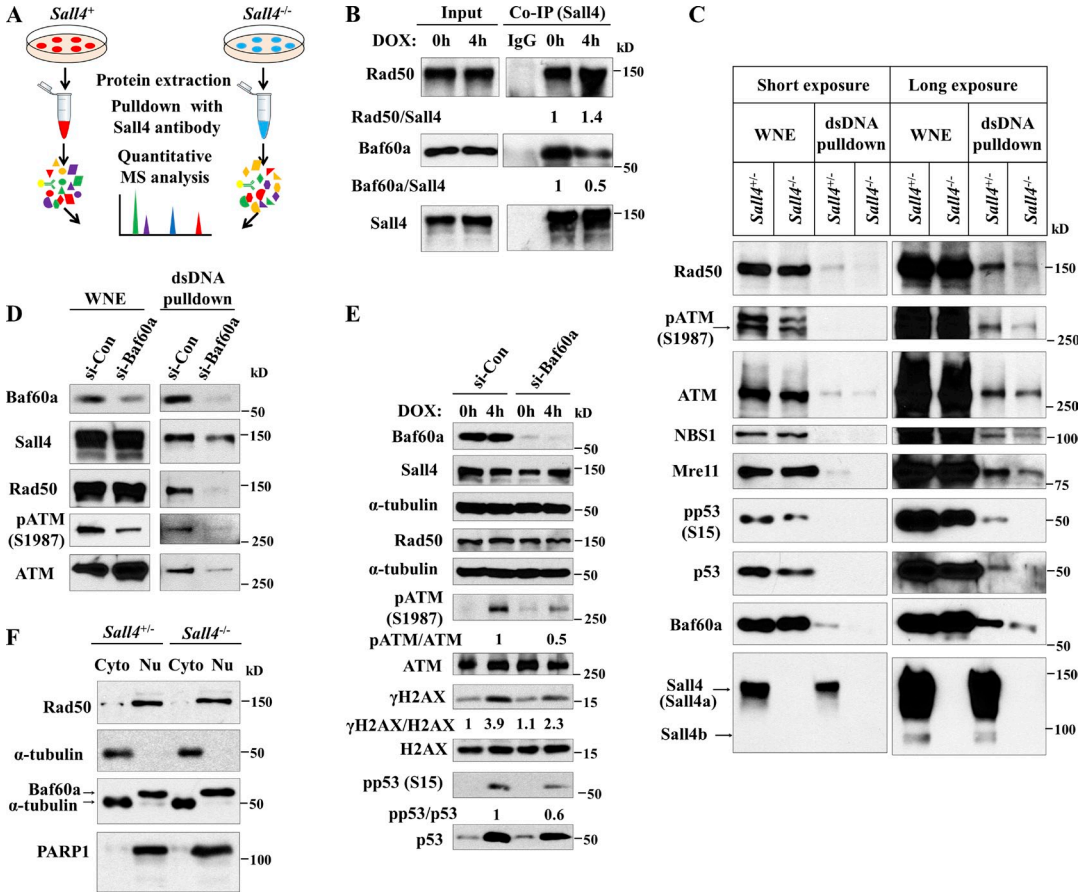

Figure 3. **Sall4 and Baf60a are required for recruiting or stabilizing MRN complex at sites of DNA DSBs.** (A) Schematic overview of mass spectrometric analysis for proteins interacting with Sall4 in ESCs. (B) The interaction between Sall4 and Rad50 or Sall4 and Baf60a was confirmed by coimmunoprecipitation (Co-IP). The samples were immunoprecipitated with the anti-Sall4 antibody, and the levels of proteins in the immunoprecipitation or input were determined by Western blotting. (C) The association of various proteins with DNA DSBs in *Sall4*$^{+/-}$ and *Sall4*$^{-/-}$ ESCs treated with 0.5 µM DOX for 4 h was determined by the linear dsDNA pull-down assay. The levels of proteins in the input whole nuclear extract (WNE) and DSB pull-down were determined by Western blotting. Short (left) and long (right) exposure of the same blots are shown. (D) Silencing of Baf60a reduces the association of Sall4, Rad50, and ATM with DNA DSBs in ESCs treated with DOX. The protein levels of Sall4, Rad50, and ATM in the whole nuclear extract input and the linear dsDNA pull-down were determined by Western blotting. (E) Silencing of Baf60a impairs the ATM activation in ESCs after DOX treatment. (F) Nuclear (Nu) and cytoplasmic (Cyto) distribution of Rad50 and Baf60a in *Sall4*$^{+/-}$ and *Sall4*$^{-/-}$ ESCs treated with 0.5 µM DOX for 4 h. si-Con, control siRNA.

posttranslational modifications and (2) ATP-dependent chromatin remodeling (Lans et al., 2012). To elucidate the mechanism by which Sall4 is recruited to the site of DNA DSBs in ESCs, we reasoned that the recruitment of Sall4 to DNA DSBs could be controlled by chromatin remodeling at the site of DSBs. We screened the Sall4-associated proteins in ESCs detected by MS for the ones involved in chromatin remodeling and identified Baf60a, which is a member of the SWI/SNF (switch/sucrose nonfermentable) complex important for pluripotency and is also implicated in DDR (Fig. 3 A and Table S2; Ho et al., 2009a,b; Lee et al., 2010; Lans et al., 2012). We confirmed the association of Sall4 with BAf60a by coimmunoprecipitation, and their interaction was decreased after DNA DSB damage, suggesting that this dynamic interaction represents a very early event during DDR in ESCs (Fig. 3 B). In support of this hypothesis, silencing of Baf60a in ESCs inhibited the recruitment of Sall4 to DNA DSBs, leading to the inefficient activation of ATM and its effector p53 and H2AX (Fig. 3, D and E). The recruitment of Baf60a to the site of DSBs was reduced in *Sall4*$^{-/-}$ ESCs after DNA DSB damage, this interdependence of Sall4 and Baf60a to be recruited to the DSBs suggest that there might be a positive feedback mechanism to stabilize this functional structure at DSB sites (Fig. 3, C and D). The reduced accumulation of Rad50 and Baf60a at the sites of DSBs in *Sall4*$^{-/-}$ ESCs was not attributed to their impaired nuclear localization because similar levels of Rad50 and Baf60a were detected in the nucleus of *Sall4*$^{+/-}$ and *Sall4*$^{-/-}$ ESCs after DNA damage (Fig. 3 F).

Sall4 links SWI/SNF-associated chromatin remodeling to MRN-dependent ATM activation

A previous study has shown that the SWI/SNF complex can be recruited to the sites of DSBs and stimulates the phosphorylation of H2AX, facilitating DSB repair by remodeling chromatin structure (Lans et al., 2012). Both the γ-H2AX phosphorylation and its colocalization with Sall4 were impaired in ESCs after DNA damage when Baf60a was silenced, further indicating that Sall4 mediates the roles of Baf60a in activating H2AX (Fig. 4 A and Fig. S2, A and B). Recent studies highlight that an increase of H3K14ac on γ-H2AX nucleosomes

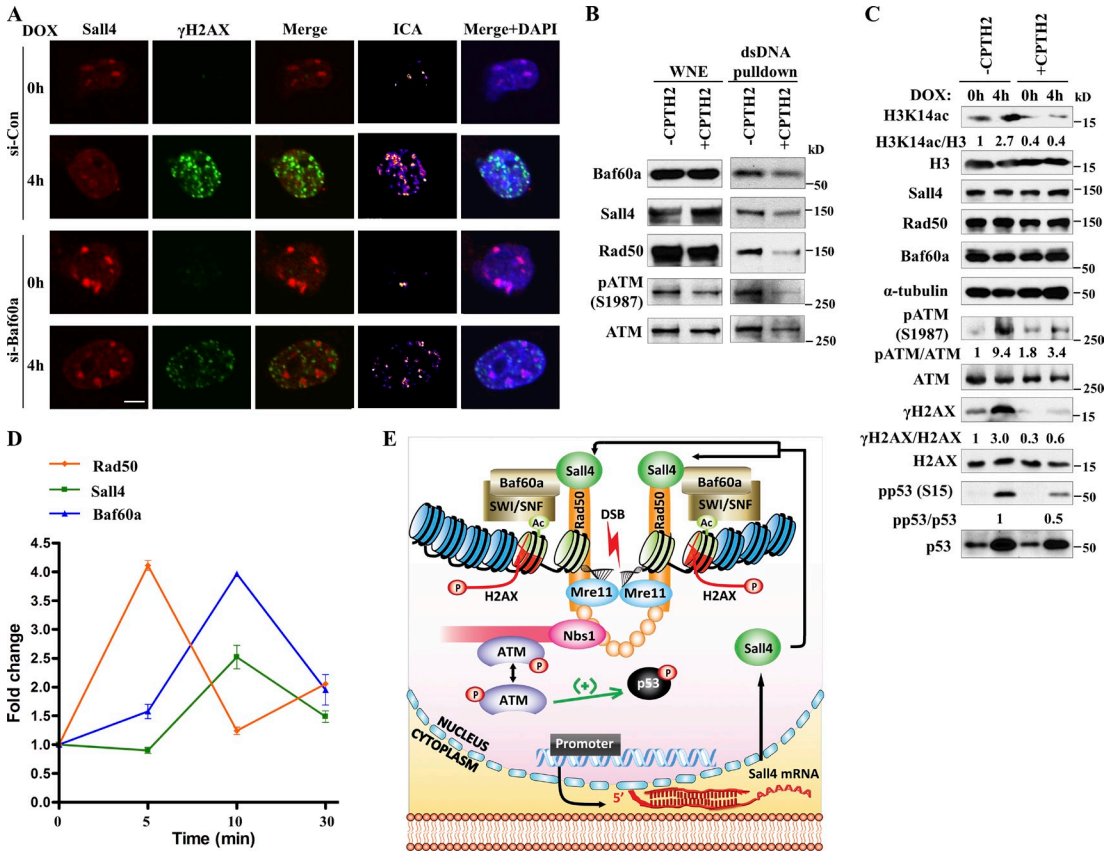

Figure 4. **Sall4 linking SWI/SNF-associated chromatin remodeling to MRN-dependent ATM activation.** (A) Silencing of Baf60a impairs the recruitment of Sall4 to γ-H2AX foci after DNA DSB damage. Nuclei are counterstained with DAPI (blue). For intensity correlation analysis (ICA), pixels from the Sall4 channel covarying positively with the corresponding signal from the γ-H2AX channel are denoted. si-Con, control siRNA. Bar, 5 µm. (B) Inhibition of H3K14ac by CPTH2 disrupts the association of Baf60a, Sall4, and ATM with DNA DSBs in the cellular extract of *Sall4*$^{+/-}$ ESCs treated with 0.5 µM DOX for 4 h. WNE, whole nuclear extract. (C) Inhibition of H3K14ac by CPTH2 in *Sall4*$^{+/-}$ ESCs impaired ATM-dependent responses to DNA DSB damage. (D) The kinetics of the recruitment of Rad50, Sall4, and Balf60a to the specific DNA DSB. ChIP analysis showed the kinetics of the recruitment of Sall4, Rad50, and Baf60a to the single I-PpoI cleavage site at chromosome 3 in *Sall4*$^{+/-}$ cells. Time denotes the minutes after the addition of 4-hydroxytamoxifen. Values are means ± SEM. (E) An illustrated model for Sall4 to function as a transducer of chromatin remodeling to ATM signaling in ESCs after DNA damage. P, phosphorylation.

offers binding sites for SWI/SNF complexes and also serves as an indicator of decondensed chromatin configuration during DDR, facilitating access to repair and signaling proteins. The histone acetyltransferase Gcn5 is responsible for H3K14ac in this process (Kim et al., 2009; Lee et al., 2010). To shed light on the function of Baf60a as a transducer of upstream chromatin remodeling to Sall4-mediated ATM signaling in DDR, the ESCs were treated with Gcn5 inhibitor CPTH2 to reduce the H3K14ac in response to DNA damage (Chimenti et al., 2009). This treatment impaired the association of Baf60a, Sall4, and Rad50 with DNA DSBs in ESCs, suggesting that H3K14ac is required for Sall4-mediated DDR (Fig. 4 B). In support of this conclusion, ATM activation was also suppressed in ESCs after DNA DSB damage in the presence of CPTH2 (Fig. 4 C). To better understand the kinetics of the recruitment of Sall4, Rad50, and Baf60a to the site of DNA DSB damage, we used an integrated DNA breakage and chromatin immunoprecipitation (ChIP) system based on tight control of the nuclear import of endonuclease I-PpoI to introduce a DNA DSB at a specific genomic site (Goldstein et al., 2013). Our findings indicate that the recruitment of Rad50 to the DNA DSB is earlier than that of Baf60a and Sall4 (Fig. 4 D). Therefore, Sall4 is not required for the recruitment of Rad50 to the site of DNA DSBs but works together with Baf60a to stabilize the MRN complex. In summary, we propose a novel model that the stemness factor Sall4 is a key transducer of DNA DSB damage-induced chromatin remodeling to MRN-dependent ATM signaling in ESCs (Fig. 4 E).

In addition to the well-established roles of Sall4 in maintaining epigenetic landscape of ESCs, our findings uncover a pivotal role of Sall4 in activating critical DDRs in ESCs. Because Sall4 is not expressed in most normal somatic cell types (Kohlhase et al., 2002), the restricted expression of Sall4 in pluripotent stem cells provides a more robust mechanism to promote efficient DDR to ensure the genomic stability of pluripotent stem cells, which is required to maintain the genomic stability of the population by giving rise to the germ cells. In addition, Northern blot analysis revealed that Sall4 is only expressed in ovary and testis but not in other tissues of adult mice, such as brain, heart, skeletal muscle, lung, liver, kidney, and spleen (Kohlhase et al., 2002). Therefore, the expression of Sall4 in the germ cells provides an additional safeguard for

genome stability of germ cells and thus the accurate genetic inheritance. Interestingly, Sall4 and Baf60a have a similar phylogenetic distribution in vertebrates (Table S1 and Fig. S3 A) and are evolutionarily conserved in placental mammalian (Fig. S3 B). Therefore, the Baf60a–Sall4 pathway could represent a common mechanism to ensure the genomic stability in mammals. In summary, our findings provide a novel mechanism for ESCs to maintain stemness and genomic stability by using one protein to control stemness-related epigenetics and DDRs.

Materials and methods

Cell preparation, culture, and treatment

All the cells were cultured at 37°C with 5% CO_2 atmosphere. The generation of *Sall4*$^{+/-}$ and *Sall4*$^{-/-}$ mouse ESCs was previously described (Yuri et al., 2009). In brief, to generate *Sall4*$^{+/-}$ ESCs, a *Sall4*-targeting vector was constructed to delete all the eight zinc finger domains of *Sall4*. *Sall4*$^{+/-}$ ESCs were electroporated with a targeting vector containing *Sall4* genomic DNA and internal ribosome entry site–blasticidin-resistance gene to generate *Sall4*$^{-/-}$ ESCs. Mouse ESCs were maintained on irradiated mouse embryo fibroblasts in KnockOut DMEM, an optimized DMEM for ESCs (Life Technologies), supplemented with 15% FBS, L-glutamine, nonessential amino acids, sodium pyruvate, β-mercaptoethanol, penicillin/streptomycin, and recombinant leukemia inhibitory factor. HEK-293T cells were grown in DMEM plus 10% FBS and penicillin/streptomycin. Mouse ESCs were either exposed to 0.5 µM DOX (Sigma-Aldrich) for a time course (0, 2, 4, and 8 h) or grown for 0.5 h after 0, 5, or 10 Gy IR. Inhibition of acetylation of H3K14 was achieved by addition of 50 µM GCN5 inhibitor, CPTH2 (cyclopentylidene-[4-(4-chlorophenyl) thiazol-2-yl]hydrazine; Sigma-Aldrich).

Western blotting and coimmunoprecipitation analysis

Cell lysates were prepared by sonication in SDS sample buffer (62.5 mM Tris-HCl, pH 6.8, 2% SDS, 10% glycerol, and 50 mM DTT), heated at 95°C for 5 min, and centrifuged for 5 min, as previously described (Kim et al., 2009), separated by 6–15% SDS-PAGE, and transferred to nitrocellulose membranes (Bio-Rad Laboratories). The membranes were developed using SuperSignal West Dura Extended Duration Substrate (Thermo Fisher Scientific). The following antibodies were used in this study: rabbit polyclonal anti–histone H3, (ab1791; Abcam), rabbit monoclonal anti–histone H2AX, (ab124781; Abcam), rabbit polyclonal anti–γ-H2AX, (2577S; Cell Signaling Technology), rabbit polyclonal anti–phospho-p53 (Ser 15; 9284L; Cell Signaling Technology), anti–rabbit IgG, HRP-linked antibody (7074S; Cell Signaling Technology), anti–mouse IgG, HRP-linked antibody (7076S; Cell Signaling Technology), mouse monoclonal anti-pATM (Ser 1981; sc-47739; Santa Cruz Biotechnology, Inc.), rabbit polyclonal anti-p53 (sc-6243; Santa Cruz Biotechnology, Inc.), mouse monoclonal anti-ATM (sc-23921; Santa Cruz Biotechnology, Inc.), mouse monoclonal anti-Baf60a (sc-135843; Santa Cruz Biotechnology, Inc.), mouse monoclonal anti–α-tubulin (T5168; Sigma-Aldrich), rabbit polyclonal anti-NBS1 (DR1033; EMD Millipore), mouse monoclonal anti-Rad50 (GTX70228; GeneTex), rabbit polyclonal anti-Mre11 (118741; GeneTex), and rabbit monoclonal anti–HP1-α, (GTX63394; GeneTex). For the coimmunoprecipitation assay, 1–3 mg of whole nuclear extract was immunoprecipitated with monoclonal antibody against Sall4 (sc-101147; Santa Cruz Biotechnology, Inc.) or HP1-α (GTX63394) followed by incubation with protein G–conjugated beads (GE Healthcare) for 4 h at 4°C. The samples were boiled with 2× SDS loading buffer for 5 min, and the amount of specific proteins was measured by Western blotting. The intensity of protein bands was quantified using ImageJ software (National Institutes of Health)

Immunofluorescence microscopy analysis

Sall4$^{+/-}$ or a mixture of *Sall4*$^{+/-}$ and *Sall4*$^{-/-}$ cells grown in a Permanox slide (Thermo Fisher Scientific) were treated with 0.5 µM DOX or 0.5 h after 10 Gy IR and subsequently fixed in 4% Paraformaldehyde Solution (Affymetrix) for 20 min at room temperature. After permeabilization with 0.4% Triton X-100, the cells were blocked in 3% BSA and then labeled with rabbit or mouse antibodies against Sall4 ab29112 (Abcam) or sc-101147, respectively; pATM (Ser 1981; 200–301-400; ROCKLAND); γ-H2AX; Baf60a; and Rad50 overnight at 4°C. The cells were further probed with Alexa Fluor 568 donkey anti–mouse IgG antibody or Alexa Fluor 488 goat anti–rabbit IgG Antibody (Life Technologies) and mounted using VECTASHIELD mounting medium with DAPI (Vector Laboratories). The images were acquired at room temperature by using 100×, 1.4 NA oil immersion objective lens in confocal microscope system (FV1000; Olympus), equipped with an inverted microscope (IX81; Olympus) and three photomultiplier tubes and driven by FluoView software (Olympus). A 405-nm diode laser, 488-nm Ar laser, and 543-nm HeNe laser were used. Acquired images were quantified with ImageJ software, by which integrated densities were measured in the area of cells. Integrated densities of the area without cells were used to background subtraction. For colocalization assessment, intensity correlation analysis was performed to highlight pixels positively covarying between two input channels using a plugin for ImageJ (http://imagej.nih.gov/ij/plugins/mbf/).

Cell cycle G_2/M checkpoint analysis

Unsynchronized *Sall4*$^{+/-}$ and *Sall4*$^{-/-}$ cells were plated on gelatin-coated dishes and treated for 1 h with 1 µM DOX (Sigma-Aldrich); untreated cells were used as a control. After treatment, the cells were harvested, washed with PBS, and fixed with 70% ethanol for 24 h at −20°C. The cells were washed with PBS, permeabilized with 0.25% Triton X-100 on ice for 15 min, stained with antibody against the mitosis marker histone H3 phosphorylated at Ser10 (Cell Signaling Technology) for 2 h at room temperature followed by incubation with Alexa Fluor 488 goat anti–rabbit antibody (Life Technologies). After a 30-min incubation, the cells were washed, resuspended in propidium iodide/RNase staining solution (Cell Signaling Technology), incubated for 15 min at room temperature, and analyzed with a flow cytometer (LSR II; BD).

Comet assay

The presence of DNA DSBs was analyzed using the Comet Assay kit from Cell Biolabs according to the manufacturer's instructions. In brief, *Sall4*$^{+/-}$ and *Sall4*$^{-/-}$ ESCs plated on gelatin-coated dishes were treated with DOX for 4 h, harvested, and washed with ice-cold PBS. Cells were resuspended at a density of 10^5 cells/ml, mixed with molten agarose at 1:10 ratio, spread onto 3-well Comet Assay slides, and solidified for 15 min at 4°C. Slides were immersed in lysis solution and electrophoresed in chilled TBE (Tris-borate-EDTA) buffer for 15 min at 20 V. Slides were then fixed in 70% ethanol and dried, and DNA was labeled with Vista Green DNA Dye. Images were captured at 10× magnification with an inverted microscope (Axiovert 40 CFL; Carl Zeiss) and analyzed using Comet Assay IV software (Perceptive Instruments); at least 100 cells were analyzed per sample.

Viral production, infection, and generation of Lenti-*Sall4* cells

All of lentivirus packaging plasmid (psPAX2, plasmid #12260, CAG promoter), envelope plasmid (pMD2.G, plasmid #12259, cytomegalovirus [CMV] promoter), the reverse tetracycline transactivator (FUW-M2rtTA, plasmid #20342, CMV promoter), and lentiviral vectors containing Sall4 (FUW-TetO-Zeo-Sall4, plasmid #40797, CMV promoter) and I-PpoI (pCL20C-ddIPpoI, plasmid #49053, Murine Stem Cell Virus promoter) were obtained from Addgene. The generation of lentiviral vectors encoding M2rtTA and Sall4 was based on a calcium phosphate–based Trono laboratory protocol with some modifications. In brief, infectious lentiviral supernatants were produced in HEK-293T cells (9×10^6 cells per 15-cm dish) cotransfected with 60 µg psPAX2, 30 µg pMD2.G, and 90 µg FUW-M2rtTA, FUW-TetO-Zeo-Sall4, or pCL20C-ddIPpoI. Supernatants were collected 48 h after transfection and concentrated using the Lenti-X concentrator (Takara Bio Inc.) and stored at −80°C. The constructs and transduction of FUW-M2rtTA and FUW-TetO-Zeo-Sall4 have been described previously (Hockemeyer et al., 2008; Buganim et al., 2012). In brief, *Sall4*$^{-/-}$ cells were infected with a constitutively active lentivirus expressing FUW-M2rtTA together with doxycycline-inducible lentivirus transducing Sall4 (FUW-TetO-Zeo-Sall4) using 5 µg/ml polybrene (EMD Millipore). *Sall4*$^{-/-}$ colonies that stably expressing Sall4 protein under the control of the tetracycline promoter, named Lenti-*Sall4*, were isolated in the presence of 50 µg/ml zeocin (Life Technologies). The colonies were expanded and screened for 4 µg/ml doxycycline (Sigma-Aldrich)-induced Sall4 expression by Western blotting.

Linear double-stranded DNA (dsDNA)–associated protein pull-down assay

Nuclear extracts were isolated from *Sall4*$^{+/-}$ or *Sall4*$^{-/-}$ ESCs treated by 0.5 µM DOX or from *Sall4*$^{+/-}$ ESCs administered by siRNAs or CPTH2 for pull-down assay as previously described (Song et al., 2007). To immobilize the biotinylated dsDNA (2 kb) that was generated by PCR amplification of pcDNA3.1 with biotinylated T7 primer and reverse primer, Dynabeads M-280 Streptavidin beads (Life Technologies) were applied according to the manufacturer's instruction. 300 ng immobilized dsDNA was mixed with nuclear or histone extracts and incubated for 30 min at room temperature followed by 2 h at 4°C with gentle rotation. The beads

were washed with ice-cold buffer D (10 mM Tris, pH 7.6, and 100 mM NaCl) and boiled for 5 min in SDS loading buffer for protein dissociation, and the dsDNA-associated proteins were analyzed with Western blotting.

siRNA transfection

For siRNA experiments in mouse ESCs, transfections of 25 nM of nontargeting pool control (indicated as si-Con) or SMARTpool siRNAs directed against Baf60a (Smarcd1; indicated as si-Baf60a) were performed using DharmaFECT 2 Transfection Reagent (Thermo Fisher Scientific) according to the manufacturer's protocol. The following pools of four siRNAs were used as si-Con and si-Baf60a: ON-TARGETplus Nontargeting Pool (D-001810-10-05; Thermo Fisher Scientific) for si-Con, 5′-GGUUUACAUGUCGACUAA-3′, 5′-UGGUUUACAUGUUGUGUGA-3′, 5′-UGGUUUACAUGUUUUCUGA-3′, and 5′-UGGUUUACAUGUUUUCCUA-3′; and ON-TARGETplus Mouse Smarcd1 (83797) siRNA SMARTpool (L-046893-01-0005; Thermo Fisher Scientific) for siBaf60a, 5′-CCUGAAAUCAAACGGGUAA-3′, 5′-CCUCAAAGGAUUCGGGAAC-3′, 5′-AAACGGAAGCUGCGAAUUU-3′, and 5′-AGAUGUGAAUGUACGGUGU-3′.

DOX sensitivity assay

Single *Sall4*$^{+/-}$, *Sall4*$^{-/-}$, and Lenti-*Sall4* ESCs were plated on mouse embryo fibroblast feeder layer in 6-well plates with a density of 3,000 cells per well. For *Sall4*$^{+/-}$ and *Sall4*$^{-/-}$ ESCs, the cells were exposed to 0.5 µM DOX in a time course 1 d after cell plating. For Lenti-*Sall4* cells, 4 µg/ml doxycycline was added into cultures. 2 d after doxycycline treatment, the cells were exposed to 0.5 µM DOX in a time course. 2 wk later, the surviving colonies were stained with crystal violet and counted.

MS

MS of Sall4 in mouse ESCs was performed as previously described (Lee, 2009). In brief, automated 2D nanoflow liquid chromatography–MS/MS analysis was performed using a tandem mass spectrometer (LTQ; Thermo Fisher Scientific) using automated data-dependent acquisition. An HPLC system (1100; Agilent Technologies) was used to deliver a flow rate of 500 nl/min to the mass spectrometer through a splitter. Chromatographic separation was accomplished using a three-phase capillary column. Using an in-house constructed pressure cell, 5 µm Zorbax SB-C18 (Agilent Technologies) packing material was packed into a fused silica capillary tubing (200 µm inside diameter [ID], 360 µm outside diameter [OD], 10 cm long) to form the first dimension reverse phase column (RP1). A similar column (200 µm ID, 5 cm long) packed with 5 µm PolySulfoethyl (PolyLC) packing material was used as the strong cation-exchange (SCX) column. A zero dead volume 1-µm filter (Upchurch) was attached to the exit of each column for column packing and connecting. A fused silica capillary (200 µm ID, 360 µm OD, 20 cm long) packed with 3.5 µm Zorbax SB-C18 packing material was used as the analytical column (RP2). One end of the fused silica tubing was pulled to a sharp tip with the ID smaller than 1 µm using a laser puller (P-2000; Sutter Instrument) as the electrospray tip. The peptide mixtures were loaded onto the RP1 column using the same in-house pressure cell. To avoid sample carryover and keep good reproducibility, a new set of three columns with the same length was used for each sample. Peptides were first eluted from RP1 column to SCX column using a 0–80% acetonitrile gradient for 150 min. Then, peptides were fractionated by the SCX column using a series of eight-step salt gradients (10, 15, 20, 30, 50, 70, and 100 mM and 1 M ammonium acetate for 20 min) followed by high resolution reverse-phase separation using an acetonitrile gradient of 0–80% for 120 min. The mass spectrometer was operated in positive ion mode with a source temperature of 150°C and a spray voltage of 1,500 V. Data-dependent analysis and gas phase separation were used. The full MS scan range of 300–2,000 mass/charge was divided into three smaller scan ranges (300–800, 800–1,100, and 1,100–2,000) to improve the dynamic range. Each MS scan was followed by four MS/MS scans of the most intense ions from the parent MS scan. A dynamic exclusion of 1 min was used to improve the duty cycle of MS/MS scans. About 200,000 MS/MS spectra were collected for each run. Raw data were extracted and searched using Spectrum Mill (version A.03.02.060b; Agilent Technologies). MS/MS spectra with a sequence tag length of 1 or less were considered as poor spectra and discarded. The filtered spectra of the MS/MS spectra were searched against the IPI (International Protein Index) database limited to mouse taxonomy v3.31 (July, 2007). The enzyme parameter was limited to full tryptic peptides with a maximum miscleavage of 2. All other search parameters were set to SpectrumMill's default settings (carbamidomethylation of cysteines, ±2.5 D for precursor ions, ±0.7 D for fragment ions, and a minimum matched peak intensity of 50%).

ChIP assay

Mouse *Sall4*$^{+/-}$ ESCs were infected by I-PpoI–expressing lentivirus and 3 d later, treated with 1 µM Shield-1 (Cheminpharma) for 3 h followed by the addition of 1 µM 4-hydroxytamoxifen (Sigma-Aldrich) as previously described (Goldstein et al., 2013). Subsequently, cells were collected for ChIP using Agarose ChIP kit (Thermo Fisher Scientific) according to the manufacturer's instructions. In brief, DNA and proteins were cross-linked in 1% formaldehyde (wt/vol; 16% formaldehyde; Thermo Fisher Scientific) and then cross-linking was stopped after 10 min at room temperature by the addition of glycine solution. Cross-linked cells were harvested for digestion of genomic DNA at 37°C with 2.5 U ChIP grade micrococcal nuclease after membrane extraction. The supernatant containing the digested chromatin was used for immunoprecipitation by specific antibodies against Sall4 (ab29112; Abcam), Rad50 (GTX70228; GeneTex), and Baf60a (sc-135843; Santa Cruz Biotechnology, Inc.), and DNA was recovered after immunoprecipitation elution. Bound DNA fragments were analyzed by real-time PCR using FastStart Universal SYBR Green Master (Rox) kit (Roche). Input DNA was used as an internal control, and normal rabbit IgG were used as negative controls. The sequences of two primer pairs (203 bp 5′ and 315 bp 3′ to the single I-PpoI cleavage site at chromosome 3, respectively) are as follows: (1) 203 bp 5′ to the I-PpoI site primer pair, forward primer, 5′-TCCGGAATGAGTCATCTTTTC-3′, and reverse primer, 5′-TTCTGTCTTGCTCCTGCAAA-3′; and (2) 315 bp 3′ to the I-PpoI site primer pair, forward primer, 5′-AAACACAACCGTCTGCTTCC-3′, and reverse primer, 5′-AAGTCATGCCAAACCTGGTC-3′.

Online supplemental material

Fig. S1 shows that *Sall4*$^{-/-}$ ESCs are hypersensitive to DNA DSB damage and impaired in ATM-dependent DDR. Fig. S2 shows that silencing of Baf60a inhibits the foci formation of γ-H2AX and the recruitment of Sall4 to DNA DSBs in ESCs. Fig. S3 presents the taxonomic trees and sequence conservation of Sall4 and Baf60a. The phylogenetic distribution of Sall4 and Baf60a is shown in Table S1, and the proteins interacting with Sall4 revealed by MS are provided in Table S2 in an online Excel file. Online supplemental material is available at http://www.jcb.org/cgi/content/full/jcb.201408106/DC1.

We thank Professor Ryuichi Nishinakamura for sharing the *Sall4*$^{+/-}$ and *Sall4*$^{-/-}$ mouse ESCs, and the University of California, San Diego Microscopy Core for imaging analysis.

This work was supported by grants from Chinese Ministry of Science and Technology (2012CB966900) and California Institute for Regenerative Medicine (RC1-00148).

The authors declare no competing financial interests.

Author contributions: J. Xiong, D. Todorova, and Y. Xu designed the experiments and analyzed the data; P.-J. Lee, Z. Shen, and S.P. Briggs performed the MS analysis. J. Xiong, D. Todorova, and N.-Y. Su executed the remaining experiments; J. Xiong and Y. Xu were responsible for the initial draft of the manuscript, whereas other authors contributed to the final edited versions.

Submitted: 29 August 2014
Accepted: 26 January 2015

References

Buganim, Y., D.A. Faddah, A.W. Cheng, E. Itskovich, S. Markoulaki, K. Ganz, S.L. Klemm, A. van Oudenaarden, and R. Jaenisch. 2012. Single-cell expression analyses during cellular reprogramming reveal an early stochastic and a late hierarchic phase. *Cell*. 150:1209–1222. http://dx.doi.org/10.1016/j.cell.2012.08.023

Chimenti, F., B. Bizzarri, E. Maccioni, D. Secci, A. Bolasco, P. Chimenti, R. Fioravanti, A. Granese, S. Carradori, F. Tosi, et al. 2009. A novel histone acetyltransferase inhibitor modulating Gcn5 network: cyclopentylidene-[4-(4′-chlorophenyl)thiazol-2-yl)hydrazone. *J. Med. Chem.* 52:530–536. http://dx.doi.org/10.1021/jm800885d

Frei, E., R. Schuh, S. Baumgartner, M. Burri, M. Noll, G. Jürgens, E. Seifert, U. Nauber, and H. Jäckle. 1988. Molecular characterization of spalt, a homeotic gene required for head and tail development in the *Drosophila* embryo. *EMBO J.* 7:197–204.

Goldstein, M., F.A. Derheimer, J. Tait-Mulder, and M.B. Kastan. 2013. Nucleolin mediates nucleosome disruption critical for DNA double-strand break repair. *Proc. Natl. Acad. Sci. USA*. 110:16874–16879. http://dx.doi.org/10.1073/pnas.1306160110

Ho, L., R. Jothi, J.L. Ronan, K. Cui, K. Zhao, and G.R. Crabtree. 2009a. An embryonic stem cell chromatin remodeling complex, esBAF, is an

essential component of the core pluripotency transcriptional network. *Proc. Natl. Acad. Sci. USA*. 106:5187–5191. http://dx.doi.org/10.1073/pnas.0812888106

Ho, L., J.L. Ronan, J. Wu, B.T. Staahl, L. Chen, A. Kuo, J. Lessard, A.I. Nesvizhskii, J. Ranish, and G.R. Crabtree. 2009b. An embryonic stem cell chromatin remodeling complex, esBAF, is essential for embryonic stem cell self-renewal and pluripotency. *Proc. Natl. Acad. Sci. USA*. 106:5181–5186. http://dx.doi.org/10.1073/pnas.0812889106

Hockemeyer, D., F. Soldner, E.G. Cook, Q. Gao, M. Mitalipova, and R. Jaenisch. 2008. A drug-inducible system for direct reprogramming of human somatic cells to pluripotency. *Cell Stem Cell*. 3:346–353. http://dx.doi.org/10.1016/j.stem.2008.08.014

Hong, Y., R.B. Cervantes, E. Tichy, J.A. Tischfield, and P.J. Stambrook. 2007. Protecting genomic integrity in somatic cells and embryonic stem cells. *Mutat. Res.* 614:48–55. http://dx.doi.org/10.1016/j.mrfmmm.2006.06.006

Jürgens, G. 1988. Head and tail development of the *Drosophila* embryo involves spalt, a novel homeotic gene. *EMBO J.* 7:189–196.

Kim, Y.C., G. Gerlitz, T. Furusawa, F. Catez, A. Nussenzweig, K.S. Oh, K.H. Kraemer, Y. Shiloh, and M. Bustin. 2009. Activation of ATM depends on chromatin interactions occurring before induction of DNA damage. *Nat. Cell Biol.* 11:92–96. http://dx.doi.org/10.1038/ncb1817

Kohlhase, J., M. Heinrich, M. Liebers, L. Fröhlich Archangelo, W. Reardon, and A. Kispert. 2002. Cloning and expression analysis of SALL4, the murine homologue of the gene mutated in Okihiro syndrome. *Cytogenet. Genome Res.* 98:274–277. http://dx.doi.org/10.1159/000071048

Koshiba-Takeuchi, K., J.K. Takeuchi, E.P. Arruda, I.S. Kathiriya, R. Mo, C.C. Hui, D. Srivastava, and B.G. Bruneau. 2006. Cooperative and antagonistic interactions between Sall4 and Tbx5 pattern the mouse limb and heart. *Nat. Genet.* 38:175–183. http://dx.doi.org/10.1038/ng1707

Lans, H., J.A. Marteijn, and W. Vermeulen. 2012. ATP-dependent chromatin remodeling in the DNA-damage response. *Epigenetics Chromatin*. 5:4. http://dx.doi.org/10.1186/1756-8935-5-4

Lee, P.J.A. 2009. Functional analysis of Sall4 in modulating embryonic stem cell fate. Electronic Theses and Dissertations. PhD thesis. University of California, San Diego, San Diego, CA. local identifier b6669710. 114 pp.

Lee, J.H., and T.T. Paull. 2007. Activation and regulation of ATM kinase activity in response to DNA double-strand breaks. *Oncogene*. 26:7741–7748. http://dx.doi.org/10.1038/sj.onc.1210872

Lee, H.S., J.H. Park, S.J. Kim, S.J. Kwon, and J. Kwon. 2010. A cooperative activation loop among SWI/SNF, γ-H2AX and H3 acetylation for DNA double-strand break repair. *EMBO J.* 29:1434–1445. http://dx.doi.org/10.1038/emboj.2010.27

Meshorer, E., and T. Misteli. 2006. Chromatin in pluripotent embryonic stem cells and differentiation. *Nat. Rev. Mol. Cell Biol.* 7:540–546. http://dx.doi.org/10.1038/nrm1938

Nagaria, P., C. Robert, and F.V. Rassool. 2013. DNA double-strand break response in stem cells: mechanisms to maintain genomic integrity. *Biochim. Biophys. Acta*. 1830:2345–2353. http://dx.doi.org/10.1016/j.bbagen.2012.09.001

Pellegrini, M., A. Celeste, S. Difilippantonio, R. Guo, W. Wang, L. Feigenbaum, and A. Nussenzweig. 2006. Autophosphorylation at serine 1987 is dispensable for murine Atm activation in vivo. *Nature*. 443:222–225. http://dx.doi.org/10.1038/nature05112

Sakaki-Yumoto, M., C. Kobayashi, A. Sato, S. Fujimura, Y. Matsumoto, M. Takasato, T. Kodama, H. Aburatani, M. Asashima, N. Yoshida, and R. Nishinakamura. 2006. The murine homolog of SALL4, a causative gene in Okihiro syndrome, is essential for embryonic stem cell proliferation, and cooperates with Sall1 in anorectal, heart, brain and kidney development. *Development*. 133:3005–3013. http://dx.doi.org/10.1242/dev.02457

Shiloh, Y. 2003. ATM and related protein kinases: safeguarding genome integrity. *Nat. Rev. Cancer*. 3:155–168. http://dx.doi.org/10.1038/nrc1011

Song, H., M. Hollstein, and Y. Xu. 2007. p53 gain-of-function cancer mutants induce genetic instability by inactivating ATM. *Nat. Cell Biol.* 9:573–580. http://dx.doi.org/10.1038/ncb1571

Stracker, T.H., and J.H. Petrini. 2011. The MRE11 complex: starting from the ends. *Nat. Rev. Mol. Cell Biol.* 12:90–103. http://dx.doi.org/10.1038/nrm3047

Sweetman, D., and A. Münsterberg. 2006. The vertebrate spalt genes in development and disease. *Dev. Biol.* 293:285–293. http://dx.doi.org/10.1016/j.ydbio.2006.02.009

Tichy, E.D., and P.J. Stambrook. 2008. DNA repair in murine embryonic stem cells and differentiated cells. *Exp. Cell Res.* 314:1929–1936. http://dx.doi.org/10.1016/j.yexcr.2008.02.007

Yang, J., W. Liao, and Y. Ma. 2012. Role of SALL4 in hematopoiesis. *Curr. Opin. Hematol.* 19:287–291. http://dx.doi.org/10.1097/MOH.0b013e328353c684

Yuri, S., S. Fujimura, K. Nimura, N. Takeda, Y. Toyooka, Y. Fujimura, H. Aburatani, K. Ura, H. Koseki, H. Niwa, and R. Nishinakamura. 2009. Sall4 is essential for stabilization, but not for pluripotency, of embryonic stem cells by repressing aberrant trophectoderm gene expression. *Stem Cells*. 27:796–805. http://dx.doi.org/10.1002/stem.14